

Peralkylated Tetrasilanes: Conformational Dependence of the Photoelectron Spectrum<sup>†</sup>Heather A. Fogarty,<sup>‡</sup> Hayato Tsuji,<sup>§</sup> Donald E. David,<sup>‡</sup> Carl-Henrik Ottosson,<sup>‡</sup> Masahiro Ehara,<sup>||</sup> Hiroshi Nakatsuji,<sup>||</sup> Kohei Tamao,<sup>\*,§</sup> and Josef Michl<sup>\*,‡</sup>

Department of Chemistry and Biochemistry, University of Colorado, Boulder, Colorado 80309-0215, Institute for Chemical Research, Kyoto University, Uji 611-0011, Japan, and Department of Synthetic Chemistry and Biological Chemistry, Graduate School of Engineering, Kyoto University, Kyoto 606-8501, Japan

Received: September 10, 2001; In Final Form: December 3, 2001

Photoelectron spectra of conformationally constrained methylated tetrasilanes **1–5** were measured, extending to the full 0–180° range the previously available 0–80° region of SiSiSiSi dihedral angles  $\omega$  provided by the monocyclic analogues **6–9**. The resulting complete picture of the conformational dependence of photoionization of the *n*-tetrasilane moiety is unfortunately somewhat distorted by differential polarizability effects of the alkyl chains used for conformational constraint. The lowest three ionization potentials are attributed to  $\sigma_{\text{SiSi}}$  bonding orbitals. The first and the third of these decrease a little as  $\omega$  goes from 0 to 180°, whereas the second one increases distinctly. Within the framework of the Koopmans' approximation, these trends in backbone MO energies agree with those computed in the HF/TZ//MP2/TZ approximation and those obtained from the simple Hückel ladder C model.

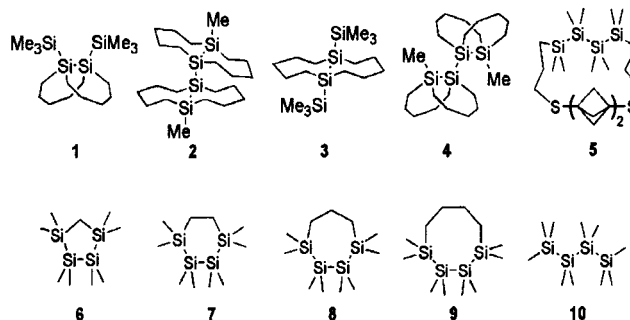
## Introduction

Much less well understood than  $\pi$  delocalization,  $\sigma$  delocalization has been of considerable interest both in its own right and because of the remarkable optical and charge-transport properties of high molecular weight linear polysilanes,  $(\text{SiRR}')_n$ .<sup>1</sup> The strong thermochromism of these materials has been attributed to conformational dependence of  $\sigma$  delocalization.<sup>1</sup> This dependence is quite striking, considering the nearly axial symmetry of individual localized  $\sigma$  bonds.

Recent advances in organosilicon synthesis and spectroscopy, and in the associated theory, have been gradually revealing the conformational dependence of electronic transitions of the tetrasilane chromophore, the shortest silicon chain subunit that involves the backbone SiSiSiSi dihedral angle  $\omega$ . The observed variation of the oscillator strengths of the two most prominent low-energy electronic transitions over the 0°  $\leq$   $\omega$   $\leq$  180° range, without much change in their excitation energies, has been attributed to a strongly avoided crossing of the two lowest excited states of B symmetry, and a similar behavior has been predicted for the lowest two excited states of A symmetry.<sup>2–5</sup> These phenomena have been rationalized by reference to molecular orbital (MO) correlation diagrams, ultimately related to the MO diagram for cis–trans isomerization of ethylene, and it would be useful to verify these correlation diagrams experimentally. Calculations<sup>6,7</sup> of the  $\sigma_{\text{SiSi}}$  bonding orbital energies as a function of the dihedral angle  $\omega$  predict that MOs transforming as the a irreducible representation of the C<sub>2</sub> symmetry group would be destabilized as  $\omega$  increases from 0 to 180° and those transforming as the b representation would be stabilized, in agreement with the simple ladder C model,<sup>7</sup> which attributes these trends to vicinal interactions.

In a previous report,<sup>8</sup> the expected conformational dependence of *n*-tetrasilane ionization potentials was confirmed in the 0°  $\leq$   $\omega$   $\leq$  80° range of dihedral angles by measuring photoelectron spectra of the methylated monocyclic tetrasilanes **6–9**, each of which has its conformation constrained to a narrow range of dihedral angles by incorporation within a five- to eight-membered ring. Because the bulk of the expected changes should occur in the 80 to 180° region, regret was expressed that *n*-tetrasilanes with such dihedral angles were not known, except as a complex and uninformative conformer mixture<sup>2</sup> in the case of *n*-Si<sub>4</sub>Me<sub>10</sub> (**10**). Recent synthetic advances have now opened access to the full range of tetrasilane conformations.<sup>4,5,9,10</sup> Bicyclic disilane structures can be used to control the conformation to be syn, ortho or anti,<sup>4,5</sup> and [*n*]staffane “molecular racks” enforce an extended anti geometry.<sup>9,10</sup>

In the present paper, we complete the “experimental MO correlation diagram” of *n*-tetrasilane ionization potentials for the full dihedral angle  $\omega$  range from 0 to 180°, based on photoelectron spectra of a series of constrained tetrasilanes and Koopmans' theorem, and identify an inherent limitation of the concept. We have also computed the optimized geometries of the tetrasilanes at an improved level of theory (MP2/TZ). In a separate paper, we plan to present the results of a similar examination of an “experimental state correlation diagram” based on measurement of various properties of electronic excited states.



<sup>†</sup> Part of the special issue “Noboru Mataga Festschrift”.

<sup>‡</sup> Department of Chemistry and Biochemistry, University of Colorado.

<sup>§</sup> Institute for Chemical Research, Kyoto University.

<sup>||</sup> Department of Synthetic Chemistry and Biological Chemistry, Graduate School of Engineering, Kyoto University.

**TABLE 1: Calculated Geometry and Observed<sup>a</sup> and Calculated<sup>b</sup> Photoelectron Spectra of 1–10**

compd	peak energy <sup>a</sup> or negative orbital energy – 0.95 <sup>b</sup> (eV)					MP2/TZ geometry			
	1 $\sigma_{\text{SiSi}}$	2 $\sigma_{\text{SiSi}}$	3 $\sigma_{\text{SiSi}}$	4 $\sigma_{\text{SiC}}$	5 $\sigma_{\text{SiC}}$	$\omega$ SiSiSiSi	$\angle$ SiSiSi/deg	terminal SiSi/Å	internal SiSi/Å
<b>1</b>	7.8	8.2	8.9	9.4	9.5	16.7	118.4	2.356	2.366
	7.96	8.27	9.19	9.62	9.66				
<b>2</b>	7.7	8.3	8.6	9.2	9.5	98.5	115.1	2.355	2.412
	7.72	8.39	8.77	9.49	9.57				
<b>3</b>	7.8	8.6	8.7	9.4	9.9	180.0	118.8	2.378	2.351
	7.78	8.76	8.83	9.52	9.83				
<b>4</b>	7.6	8.4	8.7	9.3	9.5	180.0	112.3	2.362	2.350
	7.57	8.66	8.83	9.49	9.58				
<b>5<sup>c</sup></b>	8.0	8.9	9.1	9.6	9.9	174.0	113.8	2.371	2.361
	~7.8	9.22	9.32	9.50	9.86				
<b>6</b>	7.9	8.5	~9.3	9.8	10.2	0.0	100.1	2.364	2.364
	7.62	8.39	9.44	9.68	10.29				
<b>7</b>	8.0	8.4	~9.4	9.8	10.2	38.7	104.9	2.352	2.347
	7.81	8.27	9.65	10.01	10.13				
<b>8</b>	8.0	8.6	9.2	9.8	10.2	56.1	106.0	2.364	2.346
	7.73	8.52	9.39	9.96	10.16				
<b>9</b>	8.0	8.6	9.2	9.7	9.9	82.0	115.0	2.357	2.358
	7.85	8.60	9.40	9.92	10.04				
<b>10</b>	~8.0	~9.0	~9.2	~10.2	~10.5				
<b>t</b>	7.71	9.39	9.71	11.45	11.56	162.1	111.0	2.353	2.353
<b>o</b>	7.88	9.05	9.88	11.51	11.55	91.5	113.0	2.354	2.358
<b>g</b>	7.97	8.87	10.00	11.48	11.57	54.3	114.6	2.354	2.352

<sup>a</sup> Roman. <sup>b</sup> Italic; Koopmans' theorem with additive constant,  $-\epsilon(\text{MO}) - 0.95$  eV. <sup>c</sup> Calculated and experimental energies of the sulfur lone pair ionizations are not included.

## Experimental Part

**Materials and Spectra.** Tetrasilanes **1–4** were prepared according to literature procedures<sup>4,11</sup> and purified by careful distillation or recrystallization. The [2]staffane racked tetrasilane **5** was prepared by a two-step photochemical abridgement from the known<sup>9</sup> racked hexasilane and purified by high-pressure liquid chromatography;<sup>10</sup> synthetic details will be reported elsewhere. Syntheses and purification of **6–9** have been described.<sup>8</sup> Photoelectron spectra were measured on a home-built instrument similar to a Perkin-Elmer model PS-18. Resolution was about 30 meV. For measurements on **1–5**, sample inlet and target chamber systems were heated to 113–173 °C, depending on the molecule.

**Calculations.** Ab initio calculations were performed on an IBM RS-6000–590, HP Exemplar S2000, or an HPC–PA264U computer with the Gaussian98<sup>12</sup> program. Geometry optimization was started at the HF/3-21G(d) level and was followed by frequency analysis. Further optimizations were performed at the MP2/6-31G(d) and then at the MP2/TZ [6-311G(d) on Si, 6-31G(d) on C and S, and 6-31G on H] level.

## Results

**Molecular Geometries.** Representative features of MP2/TZ optimized geometries of tetrasilanes **1–10** are listed in Table 1. For each of the tetrasilanes **7–9** several conformers with dihedral angle ranges of 12–32° were found previously<sup>8</sup> at the HF/3-21G(d) level and had nearly identical MO energies. Starting from all these conformers we found only one stable conformer for each molecule at the MP2/6-31G(d) level. Its geometry was then optimized further at the MP2/TZ level. This geometry refinement resulted in only minor changes in the silicon backbone dihedral angle  $\omega$  relative to the previously<sup>8</sup> available values.

The SiSiSiSi dihedral angles  $\omega$  were found to be 16.7° for **1**, 98.5° for **2**,<sup>13</sup> 180° for **3** and **4**, and 174.0° for **5**, which correspond to the syn, ortho, and three anti conformers,<sup>14</sup> respectively. Molecules **6–9**, with SiSiSiSi backbone dihedral angles of 0°, 38.7°, 56.1°, and 82.0°, provide access to syn,

cisoid, gauche, and ortho conformers, respectively. The SiSiSi valence angles  $\delta$  of **1–9** vary considerably from the average values of 110–115° found in the transoid, ortho, and gauche conformers of the permethylated tetrasilane, **10t**, **10o**, and **10g**, and range from 100.1° in **6** to 118.8° in **3**. In these structurally constrained molecules,  $\delta$  does not vary smoothly with  $\omega$  but is strongly influenced by the detailed nature of the constraining structural framework. SiSi bond lengths are affected, too, but the variation from the average length of 2.35 Å is mostly only moderate (–0.01 to +0.06 Å).

**Photoelectron Spectra.** The 6.5–12 eV regions of the new He(I) photoelectron spectra of conformationally constrained tetrasilanes **1–5** and the previously published<sup>8</sup> spectra for **6–10** are shown in Figure 1. The ionization potentials listed in Table 1 were read off as indicated by the correlation lines shown, with an accuracy limited by peak width and overlap. In several instances, particularly for the fourth and fifth ionization potentials, they are only a tentative guess. Three bands associated with  $\sigma_{\text{SiSi}}$  bonding orbitals are expected below ~9.5 eV, and these are of primary interest to us. At somewhat higher energies, ionizations from the  $\sigma_{\text{SiC}}$  bonding orbitals are dominant.

The three ionizations from SiSi bonds are clearly evident in the spectra, but they rarely occur as three well-defined peaks (Figure 1). In the spectra of **1**, **6**, and **7**, the first two peaks are close enough that the lower one appears only as a shoulder on the upper one. In the spectrum of **5**, ionization from the lone pairs of the two sulfur atoms through which the chain is attached to the rack, expected<sup>15</sup> to produce peaks at 8.0 and 10.0 eV, obscures the first peak. In the spectra of **6**, **7**, and **9**, the third peak appears only as a shoulder on the more intense higher energy band. In **2–5** only one peak appears in the region where the second and third ionizations are expected from interpolation and from calculations, presumably due to overlap. The peaks of the floppier molecules **2** and **4** are slightly broader than the others. The most representative spectrum of a true anti tetrasilane is probably that of **3**, with a first ionization at 7.8 eV and presumably two nearly isoenergetic ionizations near 8.8 eV. The spectrum of the free chain **10**, with its mixture of t, o, and g

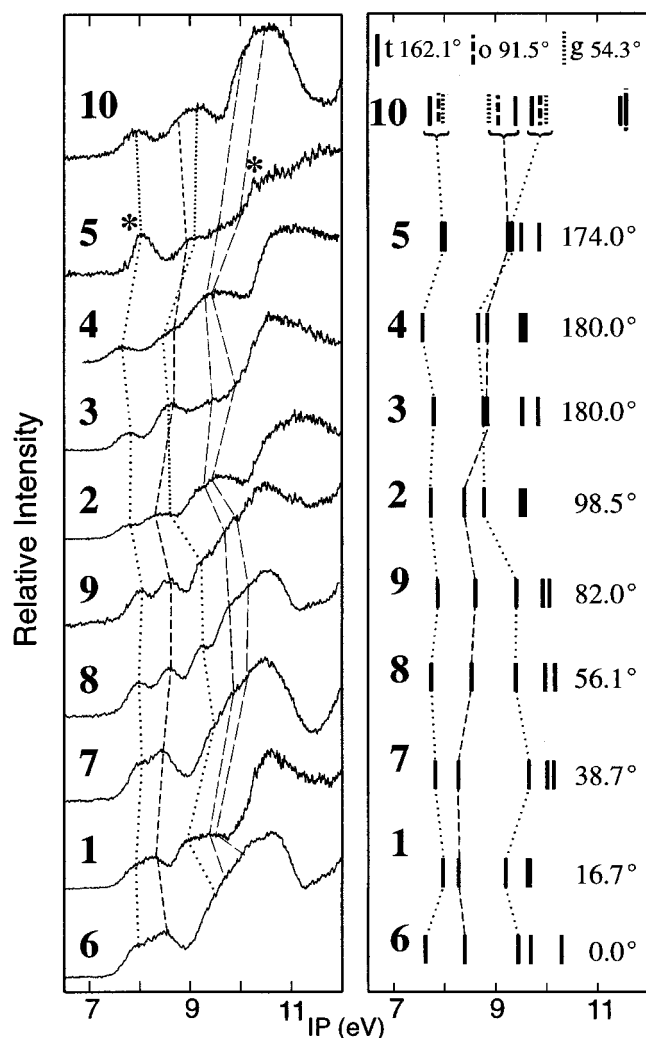


**Figure 1.** Photoelectron spectra of **1–10**: Left, measured; right, calculated (HF/TZ, Koopmans' theorem), optimized dihedral angles  $\omega$  are given. Sulfur lone pair ionization peaks are marked with an asterisk; calculated energies of sulfur lone pair ionizations are not shown.

conformers, is included for comparison, but is not particularly instructive. Although there is no experimental evidence for the calculated separate existence of more than two conformers of **10**,<sup>2</sup> all three calculated conformers of the closely related tetrasilane,  $\text{Si}_4\text{Cl}_{10}$ , have been observed,<sup>16</sup> and there is little doubt that the computational result for **10** is correct as well.

Ionization potentials of **1–10** calculated using Koopmans' theorem are collected in Table 1 and shown in Figure 1. Figure 2 shows  $\sigma_{\text{SiSi}}$  orbital energies from the photoelectron spectra of **1–10** and the MO energies for **10** calculated as a function of the SiSiSiSi dihedral angle  $\omega$ ; in these calculations,  $\omega$  was increased from 0 to 180° in 20° increments and frozen, and all other geometry variables were optimized.

## Discussion

Unlike the free chain **10**, **1–9** have their geometries constrained to a specific conformation and offer an opportunity to map out the effect of geometrical variation on tetrasilane ionization energies. In the bicyclic molecules **1** and **3**, two pentamethylene tethers, and in **5**, the racking rod, preserve a rigid silicon backbone. The optimized geometries calculated for **1** and **3** at the fairly reliable MP2/TZ level indicate that these molecules, which cannot change the SiSiSiSi backbone dihedral

angle due to inclusion of the internal SiSi bond as the bridge of a bicyclododecane unit, instead increase the SiSiSi valence angles to values above 118° to reduce steric interactions. These interactions occur between the methyl groups of one and the other terminal silicons in **1**, and between terminal methyl groups and ring methylene groups in **3**. The SiSi bond lengths are not substantially increased in **1**, but in **3** the terminal SiSi bonds are 0.02 Å longer than average. Additional evidence for very restrictive steric interactions in **1** is provided by the presence of one eclipsed CCCC dihedral angle of 120° in each seven-membered ring. In the previously studied monocyclic tetrasilanes **6–9**, the constraint on the tetrasilane backbone is less severe, except that the SiSiSi valence angle  $\delta$  is reduced to 100.1° in **6** and opened to 115° in **9**.

Finally, the rather weak constraint imposed on the central Si(2)–Si(3) bond in tetracyclic structures **2** and **4** is likely to allow facile deviation from their ortho and anti conformations, respectively, in line with the increased width of peaks in their spectra. Each of the four pentamethylene linkers is attached to a terminal Si and the adjacent internal Si, and conformational movement about the internal SiSi bond is not directly constrained by inclusion in bicyclic rings. Instead, steric interaction between pairs of rings limit the range of the SiSiSiSi dihedral angle  $\omega$ . The internal SiSi bond in **2** is extended to 0.06 Å above the average value, presumably in order to reduce the methylene–methylene interactions between rings, which increase when  $\omega$  is reduced. As in **3**, the rings are strained and there is one eclipsed C–C bond pair in each of the four seven-membered rings of **2**.

The variation of the dihedral angle  $\omega$  is the most obvious geometrical change in the series **1–9**, but it is important to ask whether the concomitant changes of other geometrical parameters could invalidate any attempt to interpret the spectral changes within the series in terms of  $\omega$  alone, with only negligible perturbations from other factors. The variation of the valence angles  $\delta$  is the most obvious such factor (Table 1), and prior computational work<sup>17</sup> on  $\text{Si}_3\text{H}_8$  indicates that it may affect the ionization potentials by as much as 0.1 eV. However, we have not found much discernible correlation between calculated or experimental ionization potentials and  $\delta$ .

The clearest trend in Figure 1 is the increasing energy difference between the first and second ionization potential, and the decreasing energy difference between the second and third ionization potential as the SiSiSiSi dihedral angle varies from 0 to 180°. The first ionization potential decreases slightly from 7.9 to 7.6 eV and the third ionization potential decreases from 9.3 to 8.7 eV as the dihedral angle increases from the syn to the anti conformation, whereas the second ionization potential increases from 8.2 to 8.9 eV. This was already predicted by HF/3-21G(d) calculations<sup>8</sup> using Koopmans' theorem, and is illustrated in Figure 2 at the HF/TZ level.

This result is easily rationalized using the ladder C model<sup>17</sup> and first-order perturbation theory. The  $\sigma_{\text{SiSi}}$  bonding orbitals in a tetrasilane can be described as shown in the computed (HF/TZ) orbital energy diagram of **10** (Figure 2), and their labels in the order of decreasing energy are a, b, and a, respectively, for  $C_2$  symmetry. Only the vicinal resonance integral  $\beta_{1,4}$  depends on  $\omega$ , and it is negative at the syn-periplanar limit and positive at the anti limit. The first and third orbitals, which are of a symmetry, are therefore a little stabilized by the vicinal interaction in the syn limit and destabilized in the anti limit, and the opposite is true for the second orbital, which is of b symmetry. The larger amplitude of the b symmetry orbital on the  $\text{sp}^3$  hybrids involved in the vicinal interaction causes it to

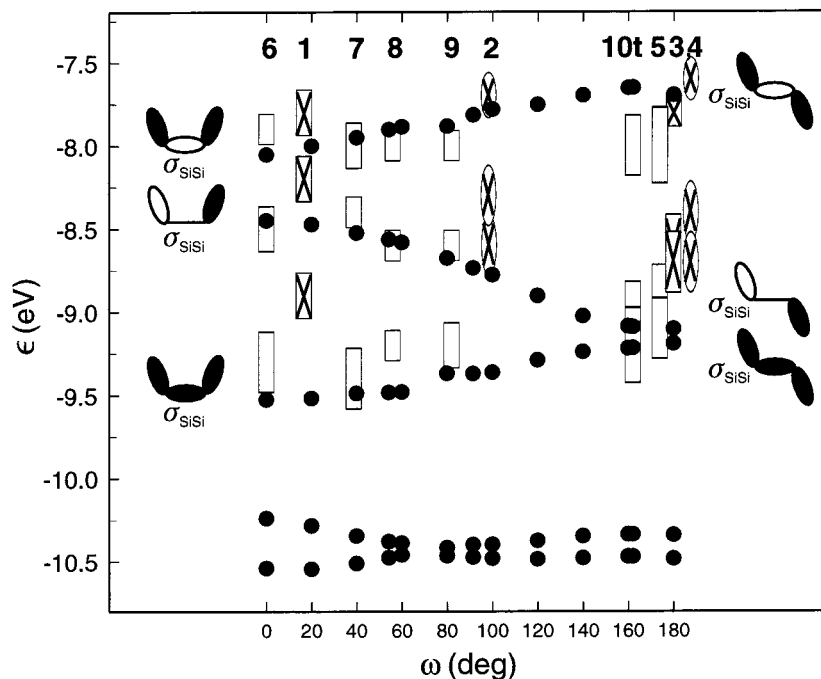


**Figure 2.** HF/TZ MO energies of **10** (●), shifted to less negative values by 0.95 eV, as a function of dihedral angle  $\omega$  (with all other geometry variables optimized). Orbital energies estimated from photoelectron spectra (Koopmans' theorem) plotted against the calculated dihedral angles for **1** and **3** (crossed rectangles), **2** and **4** (offset, crossed ellipses), **5** – **10t** (plain rectangles).

be stabilized much more than the a symmetry orbitals are destabilized as the dihedral angle approaches 180°. In fact, the effect on the latter is barely outside of the experimental uncertainties. However, the agreement of the “experimental correlation diagram” with the one expected for optimal geometries of the free chain of **10** (Figure 2) is far from perfect in that the new points for **1**–**4** do not fit the lines established by **5**–**9**, because their ionization potentials are too low.

The trends shown by the experimental ionization potentials are quite well reproduced by those computed in the Koopmans' approximation (Figure 1), although their absolute values are shifted by nearly 1 eV (Table 1). This suggests that it is not the variation in  $\delta$  but rather, the number of the larger alkyl groups in the otherwise permethylated tetrasilanes that significantly affects the energy and even the ordering of the MOs. This can be viewed as simply an effect of additional bulk of polarizable matter stabilizing the charge on the tetrasilane radical cation.<sup>18</sup>

One can classify the tetrasilanes **1**–**9** into three groups based on the number of methylene linkers present. One linker, containing varying numbers of methylene groups, is present in **5**–**9**; two linkers, each containing five methylene groups, are present in **1** and **3**; and four linkers, each also containing five methylene groups, are present in **2** and **4**. Each linker replaces two C–H bonds in *n*-Si<sub>4</sub>Me<sub>10</sub> with two C–C bonds, increasing the electron donating ability of the substituent. This pushes up the energy of the Si–C bond orbitals, which in turn interact more strongly with the tetrasilane SiSi bond orbitals, raising their energy as well. The mixing should then be reflected in the amplitudes that the top three MOs have on the adjacent carbon atoms, and this indeed is what we find. The effect on the second Si bonding MO of a symmetry is particularly significant. This argument would then suggest that attempts to set up “experimental correlation diagrams” require meticulous attention to providing strictly identical environments: replacement of small alkyl groups by larger ones is not innocent. This is already apparent from a comparison of the ease of ionization of the Si–Si bond in Si<sub>2</sub>Me<sub>6</sub> and Si<sub>2</sub>Et<sub>6</sub>.<sup>19</sup> One can hope that this high sensitivity to what would appear to be minor structural

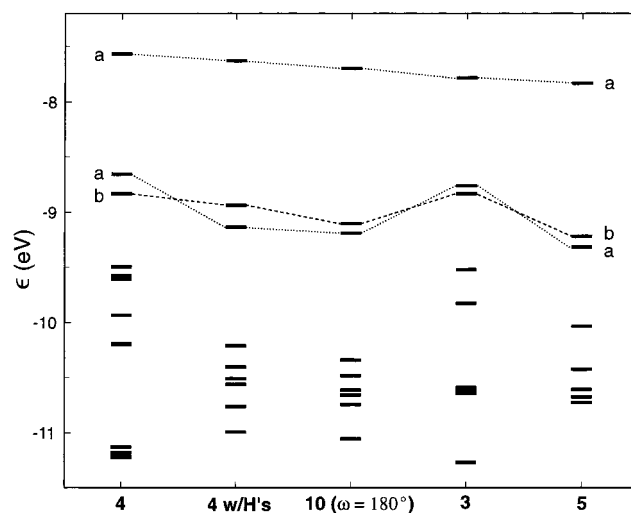


**Figure 3.** HF/TZ MO energies of **4**, **4** with the  $\beta$  and  $\gamma$  methylene groups of the rings replaced with hydrogens, **10** optimized with the SiSiSiSi backbone dihedral angle  $\omega$  frozen at 180°, **3** and **5**. Energies of the sulfur lone pair MOs in **5** are not included. C<sub>2</sub> group symmetry labels are given for the  $\sigma_{\text{SiSi}}$  MOs.

details in unimportant parts of the molecule would be reduced or absent in the experimental “state correlation diagram”, in which the ground as well as the excited states are electrically neutral.

We have verified this discouraging conclusion concerning “experimental MO correlation diagrams” by calculations on model systems. Upon replacement of the central trimethylene portion of the linkers in **4** with hydrogens, keeping the geometry otherwise constant, the calculated HF/TZ energy of the second a symmetry orbital decreased by 0.5 eV (Figure 3). Thus the methylene linkers in **3** and **4** are responsible for the surprising switch in the order of the second and third  $\sigma_{\text{SiSi}}$  bonding orbitals in these two *anti*-tetrasilanes ( $\omega = 180^\circ$ ) to a, a, b as opposed to the a, b, a order calculated for **5** and **10** ( $\omega = 180^\circ$ ). In **3**, which belongs to the class of constrained tetrasilanes with two



methylene linkers, the  $\sigma_{\text{SiSi}}$  bonding orbital energies are pushed up as in **4**, but the b symmetry orbital energy is the same as in **4** while the a symmetry orbital energies are increased slightly less (Table 1 and Figure 3). In **5**, which contains only one linker, the order of the second and third  $\sigma_{\text{SiSi}}$  bonding orbitals agrees with that calculated for **10**, and the MO energies decrease only slightly from those of **10t** (Figure 1 and Table 1). In **2**, which is constrained by four methylene linkers, the MO ordering is a, b, a as expected, but the calculated second and third MO energies are increased 0.2 and 0.6 eV, respectively, relative to the corresponding ionization potentials in **9**, although these two molecules have the same  $\delta$  and terminal bond lengths, a difference in  $\omega$  of only 17°, and a 0.05 Å internal bond length difference (Table 1). A decrease in the calculated  $\sigma_{\text{SiSi}}$  ionization potentials of **1** relative to **6** and **7** is also seen and attributed to the two methylene linkers it bears.

Geometry changes other than variation of the SiSiSiSi backbone dihedral angle  $\omega$  and the number of methylene linkers may produce small (0.1–0.2 eV) changes in the energy of each of the  $\sigma_{\text{SiSi}}$  orbitals. This effect is seen when comparing the model for **4** in which hydrogens have replaced the  $\beta$  and  $\gamma$  methylene groups in each ring, and **10** optimized at  $\omega = 180^\circ$  (Figure 3), as they both have the same connectivity and  $\omega = 180^\circ$ . A comparison of the first and third ionization potentials calculated for **8** and **10g** (Table 1 and Figure 1) is also useful because the differences between these two gauche compounds, the presence of one methylene linker and the  $\delta$  value, should have opposite effects. The methylene linker in **8** should decrease the first and third  $\sigma_{\text{SiSi}}$  ionization potentials while the reduction of the valence angle  $\delta$  from 114.6° in **10g** to 106° in **8** should increase them, if their behavior is similar to that calculated for trisilane.<sup>17</sup> The ionization potentials calculated for **8** are lower by 0.2 and 0.6 eV, respectively, than those of **10g**, which indicates that the stabilizing effect of the methylene linker is greater than the destabilizing effect of the change in  $\delta$ .

## Conclusions

The ionization potentials of the nine conformationally constrained tetrasilanes examined are in qualitative agreement with MO energies using Koopmans' theorem and the HF/TZ//MP2/TZ level of calculation, although their absolute values are off by about 1 eV. Correlation and reorganization effects that lie beyond Koopmans' approximation are responsible for additional small discrepancies, such as the surprisingly low sensitivity of the observed first and third ionization potential to changes in the dihedral angle  $\omega$ . However, these effects are not sufficiently large to invalidate an analysis based on Koopmans' theorem.

The variation of the ionization potential with the backbone dihedral angle conforms only roughly to expectations based on

calculations for the free Si<sub>4</sub>Me<sub>10</sub> chain and on the ladder C model, and many points deviate significantly from the anticipated smooth behavior. This is not primarily due to the modification of valence angles and bond lengths in the tetrasilane backbone imposed by the steric constraints; the main cause is the presence of a varying number of methylene linkers in different members of the series. A more uniformly alkylated series of tetrasilanes would be necessary to produce a smooth "experimental MO energy correlation diagram".

**Acknowledgment.** Financial support by the USARO (DAAG-55-98-1-0310), NSF (CHE-9819179) and from the Ministry of Education, Science, Sports, and Culture of Japan (09239103) is gratefully acknowledged. We thank Dr. Y. Murata and Prof. K. Komatsu for the use of their computer for some of the calculations, and Prof. R. Crespo for helpful discussions.

## References and Notes

- (1) For reviews see (a) Miller, R. D.; Michl, J. *Chem. Rev.* **1989**, *89*, 1359. (b) Michl, J.; West, R. In *Silicon-Based Polymers: The Science and Technology of their Synthesis and Applications*; Jones, R. G.; Ando, W.; Chojnowski, J., Eds.; Kluwer Academic Publishers: Dordrecht, The Netherlands, 2000, p 499.
- (2) Albinsson, B.; Teramae, H.; Downing, J. W.; Michl, J. *Chem. Eur. J.* **1996**, *2*, 529.
- (3) Imhof, R.; Teramae, H.; Michl, J. *Chem. Phys. Lett.* **1997**, *270*, 500.
- (4) Tamao, K.; Tsuji, H.; Terada, M.; Asahara, M.; Yamaguchi, S.; Toshimitsu, A. *Angew. Chem., Int. Ed.* **2000**, *39*, 3287.
- (5) Tsuji, H.; Toshimitsu, A.; Tamao, K.; Michl, J. *J. Phys. Chem. A* **2002**, in press.
- (6) Ensslin, W.; Bergman, H.; Elbel, S. *J. Chem. Soc., Perkin Trans. 2* **1975**, *71*, 913. Bock, H.; Ensslin, W.; Fehér, F.; Freund, R. *J. Am. Chem. Soc.* **1976**, *98*, 668. Mintmire, J. W.; Ortiz, J. V. *Macromolecules* **1988**, *21*, 1191. Ortiz, J. V.; Mintmire, J. W. *J. Am. Chem. Soc.* **1988**, *110*, 5422. Apeloig, Y.; Danovich, D. *Organometallics* **1996**, *15*, 350.
- (7) Teramae, H.; Michl, J. *Mol. Cryst. Liq. Cryst.* **1994**, *256*, 149. Plitt, H. S.; Downing, J. W.; Raymond, M. K.; Balaji, V.; Michl, J. *J. Chem. Soc., Faraday Trans.* **1994**, *90*, 1653.
- (8) Imhof, R.; Antic, D.; David, D. E.; Michl, J. *J. Phys. Chem. A* **1997**, *101*, 4579.
- (9) Mazières, S.; Raymond, M. K.; Raabe, G.; Prodi, A.; Michl, J. *J. Am. Chem. Soc.* **1997**, *119*, 6682.
- (10) Fogarty, H. A.; Michl, J., unpublished results.
- (11) Tamao, K.; Tsuji, H.; Toshimitsu, A. *Synlett* **2001**, 964.
- (12) Frisch, M. J., et al., Gaussian 98, revision A.6; Gaussian, Inc.; Pittsburgh, PA, 1998.
- (13) This dihedral angle is slightly larger than that found with a DFT method: see ref 4.
- (14) Michl, J.; West, R. *Acc. Chem. Res.* **2000**, *33*, 821.
- (15) Wagner, G.; Bock, H. *Chem. Ber.* **1974**, *107*, 68.
- (16) Zink, R.; Magnera, T. F.; Michl, J. *J. Phys. Chem. A* **2000**, *104*, 3829.
- (17) Ortiz, J. V.; Mintmire, J. W. *J. Phys. Chem.* **1991**, *95*, 8609.
- (18) Hansch, C.; Leo, A.; Taft, R. W. *Chem. Rev.* **1991**, *91*, 165.
- (19) Mochida, K.; Worley, S. D.; Kochi, J. K. *Bull. Chem. Soc. Jpn.* **1985**, *58*, 3389.